Journal of Inflammation Research

Dovepress
Taylor & Francis Group

Open Access Full Text Article

ORIGINAL RESEARCH

Multi-Omics Reveal the Potential Associations of *Streptococcus*, 13′-Hydroxy-Alpha-Tocopherol and Glutathione Metabolism in Children with Chronic Rhinosinusitis with Nasal Polyps

Chao Jia[1,*], Xiaoge Liu[2,3,*], Wenjing Liu[2], Xingfeng Yao[1], Xiaoxu Chen[2], Jinhao Zhao[2], Pengpeng Wang[2], Wentong Ge[2,4,5], Yang Han[2]

[1]Department of Pathology, Beijing Children's Hospital, Capital Medical University, National Center for Children's Health, Beijing, 100045, People's Republic of China; [2]Department of Otolaryngology, Head and Neck Surgery, Beijing Children's Hospital, Capital Medical University, National Center for Children's Health, Beijing, 100045, People's Republic of China; [3]The Sixth Affiliated Hospital of Harbin Medical University, Harbin Medical University, Harbin, Heilongjiang, 150081, People's Republic of China; [4]Beijing City Key Laboratory of Otolaryngology, Head and Neck Surgery, Beijing Children's Hospital, Capital Medical University, National Center for Children's Health, Beijing, 100045, People's Republic of China; [5]Department of Otolaryngology, Head and Neck Surgery, National Clinical Research Center for Respiratory Diseases, Beijing Children's Hospital, Capital Medical University, National Center for Children's Health, Beijing, 100045, People's Republic of China

*These authors contributed equally to this work

Correspondence: Wentong Ge; Yang Han, Department of Otolaryngology, Head and Neck Surgery, Beijing Children's Hospital, Capital Medical University, National Center for Children's Health, 56 NanLishi Road, Xicheng District, Beijing, 100045, People's Republic of China, Tel +86 010-5961 6391, Email gwt@bch.com.cn; hany_ent@126.com

Background: Chronic rhinosinusitis with nasal polyps (CRSwNP) in children is a clinically significant inflammatory disorder characterized by persistent symptoms and complex underlying mechanisms. This study used multi-omics approaches to investigate potential microbial and metabolic associations in pediatric CRSwNP.

Methods: Nasal secretions from 20 children with CRSwNP and 19 healthy controls were analyzed using metagenomics, untargeted metabolomics, and proteomics.

Results: CRSwNP patients showed higher microbial diversity and altered microbial communities, with increased *Streptococcus* abundance. Metabolomic sequencing revealed that 13′-Hydroxy-alpha-tocopherol was significantly upregulated in the CRSwNP group and exhibited a positive correlation with the abundance of *Streptococcus*. Proteomic sequencing revealed that proteins involved in glutathione metabolism were significantly downregulated in the CRSwNP group, with GCLM and GGCT showing a significant negative correlation with 13′-Hydroxy-alpha-tocopherol.

Conclusion: These associative findings suggest potential links among *Streptococcus*, 13′-Hydroxy-α-tocopherol, and glutathione metabolism, indicating that oxidative stress–related imbalance may contribute to pediatric CRSwNP. These results provide preliminary evidence that 13′-Hydroxy-α-tocopherol may serve as a potential biomarker for pediatric CRSwNP.

Keywords: chronic rhinosinusitis with nasal polyps, *streptococcus*, 13′-hydroxy-alpha-tocopherol, glutathione metabolism, multi-omics

Introduction

Chronic rhinosinusitis is a chronic inflammatory disease of the nasal mucosa, characterized by symptoms such as nasal congestion, rhinorrhea, facial fullness, and olfactory dysfunction, which persist for more than 12 weeks before diagnosis. The prevalence in children is 5–15%,[1] and it can be classified into two phenotypes: with or without nasal polyps. Persistent symptoms affect children's sleep, lead to poor concentration, and subsequently impact academic performance. These symptoms may also result in anxiety, depression, and other emotional disturbances, severely compromising the quality of life in affected children.[2]

https://doi.org/10.2147/JIR.S567582
Received: 27 September 2025
Accepted: 6 January 2026
Published: 25 January 2026

The upper respiratory tract is constantly exposed to environmental factors and is colonized by various microorganisms under physiological conditions, with a balanced nasal microbiota contributing to mucosal homeostasis. However, recurrent infections may alter the structure of the microbial community, promote dysbiosis, impair epithelial barrier integrity, and dysregulate mucosal immune responses, thereby contributing to chronic rhinosinusitis.[3] Prior therapies and environmental exposures may further modulate these processes.[4] Previous studies have shown that the microbial composition of pediatric CRS differs significantly from that of adult patients: phylum Actinobacteria is more prevalent in adults, whereas genera such as *Staphylococcus* and *Streptococcus* are relatively more abundant in children.[5] These differences indicate that pediatric CRS may have distinct biological characteristics, underscoring the importance of studies specifically focused on pediatric populations.

This study aims to identify differentially abundant microbial communities, metabolites, and proteins between children with CRSwNP and healthy controls through integrated microbiome analysis, untargeted metabolomics profiling, and proteomics. By combining these data, we hope to better understand the mechanisms driving pediatric CRSwNP and investigate potential therapeutic targets.

Methods

Experimental Design

This study included 20 children diagnosed with chronic rhinosinusitis with nasal polyposis (CRSwNP), who were treated at the Department of Otorhinolaryngology-Head and Neck Surgery, Beijing Children's Hospital, Capital Medical University, from September 2022 to October 2023. According to the diagnostic criteria for pediatric CRS in EPOS 2020, children in the CRSwNP group presented with the following symptoms: nasal congestion or nasal discharge (anterior/posterior nasal drip), with or without facial pain or a sensation of swelling, and with or without cough. At least two of these symptoms were present, and symptoms persisted for ≧12 weeks. All patients received 12 weeks of standardized preoperative therapy, including daily intranasal corticosteroids, twice-daily nasal saline irrigation, and oral mucolytics, with no systemic corticosteroids administered before surgery. Nasal polyps were confirmed by endoscopy and sinonasal CT. Functional endoscopic sinus surgery (FESS) was performed under general anesthesia, and patients were followed postoperatively at the outpatient clinic.

Additionally, 19 control subjects were recruited from children undergoing surgical treatment for unilateral nasal bone fractures during the same period. These subjects had no history of chronic or recurrent rhinosinusitis, allergic rhinitis, or recent (within 3 months) respiratory infection. Children with nasal bone fractures routinely underwent sinus CT scans for trauma evaluation, and combined with detailed clinical history as well as intraoperative endoscopic assessment of the nasal mucosa, this allowed reliable evaluation and confirmation of the absence of sinonasal disease. Nasal secretions were collected from the non-fractured side seven days after injury, when mucosal edema and acute-phase metabolic changes had largely resolved. All controls received standardized perioperative management at the same center.

All participants were from the same geographic region (northern China) to minimize environmental variability. Both groups of children underwent preoperative examinations, including complete blood count, allergy testing, and pulmonary function tests. To ensure comparability and minimize potential confounding factors, the baseline characteristics of the CRSwNP and Control groups were similar (Table 1). Under general anesthesia, cotton swabs and polyethylene sponges were placed in the children's nasal passages to collect nasal secretions. These samples were then stored at −80°C for further analysis. All participants received consistent preoperative care, and sample collection and storage procedures were standardized across both groups to reduce potential confounding effects of prior therapy and environmental exposures. All omics samples were collected, extracted, and processed within the same experimental batch to minimize batch effects.

The study protocol was approved by the Ethics Committee of Beijing Children's Hospital, Capital Medical University (approval number [2022]-E-215-Y). Prior to study commencement, written informed consent was obtained from the parents or legal guardians of all enrolled participants.

Table 1 Summary of Patient Characteristics

Characteristic	CRSwNP (n=20)	Control (n=19)	P-value
Age (y), mean± (SD)	10.25±1.47	10.91±2.69	0.3494
Sex (Male/Female)	15/5	14/5	1.000
BMI (Kg/m^2), mean± (SD)	18.90±3.13	19.29±2.19	0.6570
Allergy, n (%)	9 (45)	0 (0)	0.0012**
Eosinophil count (10^9/L), mean± (SD)	0.15±0.07	0.13±0.06	0.3507
Lymphocytes count (10^9/L), mean± (SD)	2.49±0.54	2.83±0.65	0.0854
Neutrophil count (10^9/L), mean± (SD)	3.71±1.42	3.51±1.19	0.6368
Lund-Mackay score, median (IQR)	8 (6–20.25)	0 (0–1)	<0.0001***
Lund-Kennedy score, median (IQR)	8 (7–10)	0 (0–0)	<0.0001***

Notes: Continuous variables are shown as mean ± SD or median (IQR) as appropriate. Categorical variables are shown as n (%). P-values were calculated using Student's *t*-test or Mann–Whitney *U*-test for continuous variables, and χ^2-test or Fisher's exact test for categorical variables; **p<0.01, ***p<0.001.
Abbreviations: CRSwNP, chronic rhinosinusitis with nasal polyps; BMI, body mass index; IQR, interquartile range; SD, standard deviation.

Microbial Metagenomics

For metagenomic sequencing, a subset of samples (10 per group) was selected using an age- and sex-matched design with additional consideration of key clinical characteristics, followed by random selection within matched strata. DNA was extracted from nasal secretion samples using the QIAamp UCP Pathogen Mini Kit (50214, Qiagen, Germany).[6] The extracted DNA was quantified using the Qubit dsDNA HS Assay Kit (Q32854, Invitrogen, USA). Libraries were constructed using the Nextera DNA Flex Kit (Illumina, San Diego, California, USA). DNA was fragmented, labeled, amplified, and purified. The Qubit dsDNA HS Assay Kit was used tomeasure the library concentration. The quality of the library was assessed using the Agilent 2100 Bioanalyzer with the High Sensitivity DNA Kit (Agilent Technologies, California, USA). The final library was sequenced using the Illumina NextSeq 550 instrument, employing a PE150 sequencing strategy. Raw data quality was assessed and filtered using FastQC software.[7] Genome assembly was performed using MEGAHIT,[8] and the results were evaluated using QUAST software. Gene-coding regions in the genome were identified using MetaGeneMark software with default parameters (Version 3.26, http://exon.gatech.edu/meta_gmhmmp.cgi). The gene translation into amino acid sequences was performed using Prokka software (v 2.6.3). Redundancy removal was performed using MMseqs2 software (https://github.com/soedinglab/mmseqs2, Version 12–113e3), with the similarity threshold set at 95% and the coverage threshold set at 90%. Species classification was performed using the NCBI Taxonomy Database, and microbial species abundance was determined based on the abundance of the corresponding genes.

Metabolomics

Non-targeted metabolite analysis was performed using liquid chromatography-mass spectrometry (LC-MS). An appropriate volume of extraction solution (methanol-acetonitrile, 1:1 v/v, internal standard concentration 20 mg/L) was added to the nasal secretion samples and subjected to ultrasonic treatment. After standing and centrifugation, the supernatant was collected and vacuum dried. Then, an appropriate volume of extraction solution (acetonitrile-water, 1:1 v/v) was added for reconstitution before analysis. The analysis was performed using the Waters Acquity I-Class PLUS ultra-high performance liquid chromatography system coupled with the Waters Xevo G2-XS QTOF high-resolution mass spectrometer, employing both positive ion and negative ion modes. The raw data collected with MassLynx V4.2 were processed using Progenesis QI software for peak extraction, alignment, and other data processing tasks. Data identification was performed using Progenesis QI software, the online METLIN database, and other public databases, with theoretical fragmentation also identified. QC samples were included throughout instrument runs to evaluate mass-spectrometry stability, and CV values were calculated to ensure analytical consistency. The m/z value deviation for the parent ion was within 100 ppm, and for the fragment ion, it was within 50 ppm. Prior to downstream analyses, biological reproducibility within each group was evaluated using Spearman rank correlation (r^2), and only datasets with high intra-group reproducibility were further analyzed. After metabolite identification and quantification, data quality was assessed.

Orthogonal partial least squares discriminant analysis (OPLS-DA) was used to identify metabolite differences between the CRSwNP and control groups, with significant features selected based on variable importance in projection scores, p-values, and $\log_2$ fold change thresholds, followed by KEGG enrichment analysis.

Proteomics

50 μg of protein was extracted from each sample for reduction treatment. After freeze-drying, the lyophilized sample was dissolved in mobile phase A (100% mass spectrometry-grade water, 0.1% formic acid), followed by centrifugation to collect the supernatant for LC-MS analysis. The mass spectrometer used was the Q Exactive HF-X instrument, operating in data-dependent acquisition (DDA) mode. The first-stage mass spectrometry scan range was m/z 350–1550, with a resolution of 120,000, AGC set to 3×10^6, and a maximum injection time of 80 ms. The top 40 parent ions were selected for higher-energy collisional dissociation to acquire second-stage mass spectrometry data, with a resolution of 15,000, AGC set to 5×10^4, a maximum injection time of 45 ms, and collision energy set at 27%. Subsequently, data-independent acquisition (DIA) mode was employed for further mass spectrometry analysis. The full scan range of the mass spectrometer was m/z 350–1500, with a resolution of 60,000, a maximum injection time of 50 ms, and collision energies set to 25.5%, 27%, and 30%. Mass spectrometry data were processed in Spectronaut software using the Pulsar module for DDA and DIA data retrieval. A spectral library was created, with database selection based on species sequencing information and the completeness of the annotations. QC samples and peak-area normalization were applied similarly to metabolomics to ensure analytical consistency, and intra-group reproducibility was assessed prior to downstream analysis. Differential protein selection followed p-value and $\log_2$FC thresholds.

Statistical Methods

All statistical analyses were conducted using SPSS version 26. Results for categorical data were expressed as percentages, and group differences were analyzed using the Chi-square test or Fisher's exact test. Normality of continuous variables was assessed using the Shapiro–Wilk test, with results presented as median ± standard deviation. Comparisons between the two groups were made using two-tailed independent samples *t*-test or the non-parametric Mann–Whitney *U*-test.

Results

Experimental Design and Clinical Data Analysis

This study included children with CRSwNP as the experimental group, with healthy controls recruited from children with nasal bone fractures who required surgical treatment and were matched for age and gender with the CRSwNP group. Due to the nasal bone trauma, all patients had completed a nasal bone CT, enabling a thorough assessment of the sinus mucosa and bone structure in the control group. Additionally, volunteers with no prior history of sinusitis were recruited. In accordance with the guidelines for the surgical timing of pediatric nasal bone fractures, these patients underwent surgery approximately 14 days after the injury.[9,10] During surgery, nasal secretions were collected by placing polyethylene glycol sponges in the middle nasal passage for metagenomic, metabolomic, and proteomic sequencing, followed by multi-omics integrated bioinformatics analysis (Figure 1).

Metagenomics

Ten nasal secretion samples from both the experimental and control groups were collected for metagenomic sequencing to identify the microbial species, quantity, and functions in nasal secretions (Table S1). According to the species diversity α analysis, the Shannon index in the CRSwNP group was higher than in the control group, indicating greater microbial species diversity in the CRSwNP group compared to the control group (Figure 2A and Table S2). Principal coordinates analysis was used to perform β-diversity analysis of microbial species in the CRSwNP and control groups. The results revealed significant differences in microbial species composition between the two groups (Figure 2B and Table S3). At the phylum level, 14 significantly different microbes were identified between the CRSwNP and control groups; at the genus level, 94 significantly different microbes were identified; and at the species level, 451 significantly different microbes were observed. Among these, we focused on the inter-group differences in microbial populations at the genus level. The abundance of 86 microbial

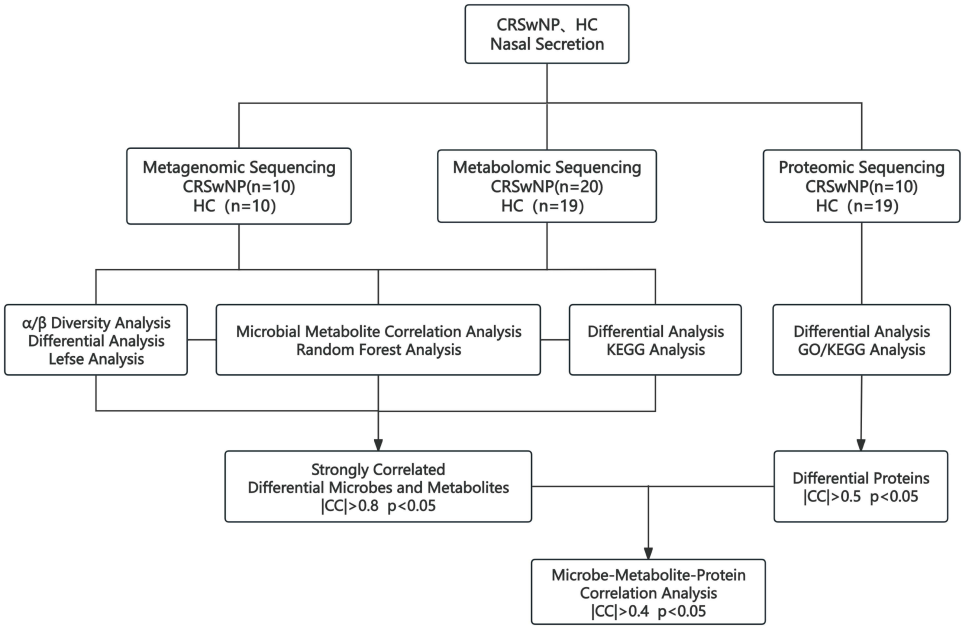

Figure 1 Study Workflow.

populations, including *Veillonella*, *Actinomyces*, *Capnocytophaga*, *Streptococcus*, *Bacteroides*, and *Prevotella*, was significantly upregulated in the CRSwNP group. In contrast, 8 microbial populations, including *Staphylococcus*, *Chlamydia*, and *Bacillus*, were downregulated in the CRSwNP group (Figure 2C–E and Table S4). Lefse analysis revealed that 17 genera, including *Actinomyces*, *Prevotella*, *Veillonella*, and *Streptococcus*, were significantly enriched in the CRSwNP group, while 9 genera, including *Staphylococcus aureus*, were significantly enriched in the control group (Figure 2F and Table S5).

Metabolomics

We collected nasal secretions from 20 CRSwNP pediatric patients and 19 healthy controls for metabolomic analysis. OPLS-DA showed $R^2Y = 0.99$ and $Q^2Y = 0.514$, indicating that the model was effective (Figure 3A and Table S6). A total of 982 differential metabolites ($p < 0.05$) were identified between the two groups, with 354 metabolites upregulated and 628 metabolites downregulated in the CRSwNP group. Metabolites such as hydroxydeoxyguanosine, Methionyl-Asparagine, Pyroglutamylglycine, 13′-Hydroxy-alpha-tocopherol, HBOA glucuronide, and 3,N(4)-Ethenodeoxycytidine were significantly upregulated in the nasal secretions of the CRSwNP group. On the other hand, PS (22:1(13z)/PGJ2), pe (22:1(13z)/PGE2), Indeloxazine, Notoginsenoside E, 3-Hydroxysebacic acid, SM (d18:1/15:0), and Vinylphosphonic acid were significantly downregulated in the CRSwNP group (Figure 3B and Table S7). KEGG enrichment analysis revealed that the differential metabolites between the two groups were significantly associated with cholesterol metabolism and primary bile acid biosynthesis pathways (Figure 3C and Table S8).

Metagenomic and Metabolomic Integrated Analysis

Principal component analysis revealed differences in microbial populations and metabolites between the CRSwNP group and the control group (Figure 4A). First, a correlation analysis was conducted between the differential metabolites in the nasal secretions of both groups and the microbial species abundance, with a threshold of CCP < 0.05 and |CC| > 0.8. A total of 24 microbial species were positively correlated with 81 metabolites, while 1 microbial species was negatively correlated with 3 metabolites (Figure 4B and Table S9). The intersection of these 84 metabolites with the inter-group differential metabolites was identified, and those with $p < 0.05$ were further analyzed using a random forest classification model, followed by ROC curve analysis. Among them, 62 metabolites had an AUC > 0.7 (Figure 4C and Table S10). The intersection of the 23 microbes and the results of the non-parametric test analysis of inter-group differential microbes yielded 15 microbes. Additionally, based on the metagenomic results and previous research reports, *Actinomyces*, *Alloprevotella*, *Streptococcus*, *Prevotella*,

https://doi.org/10.2147/JIR.S567582

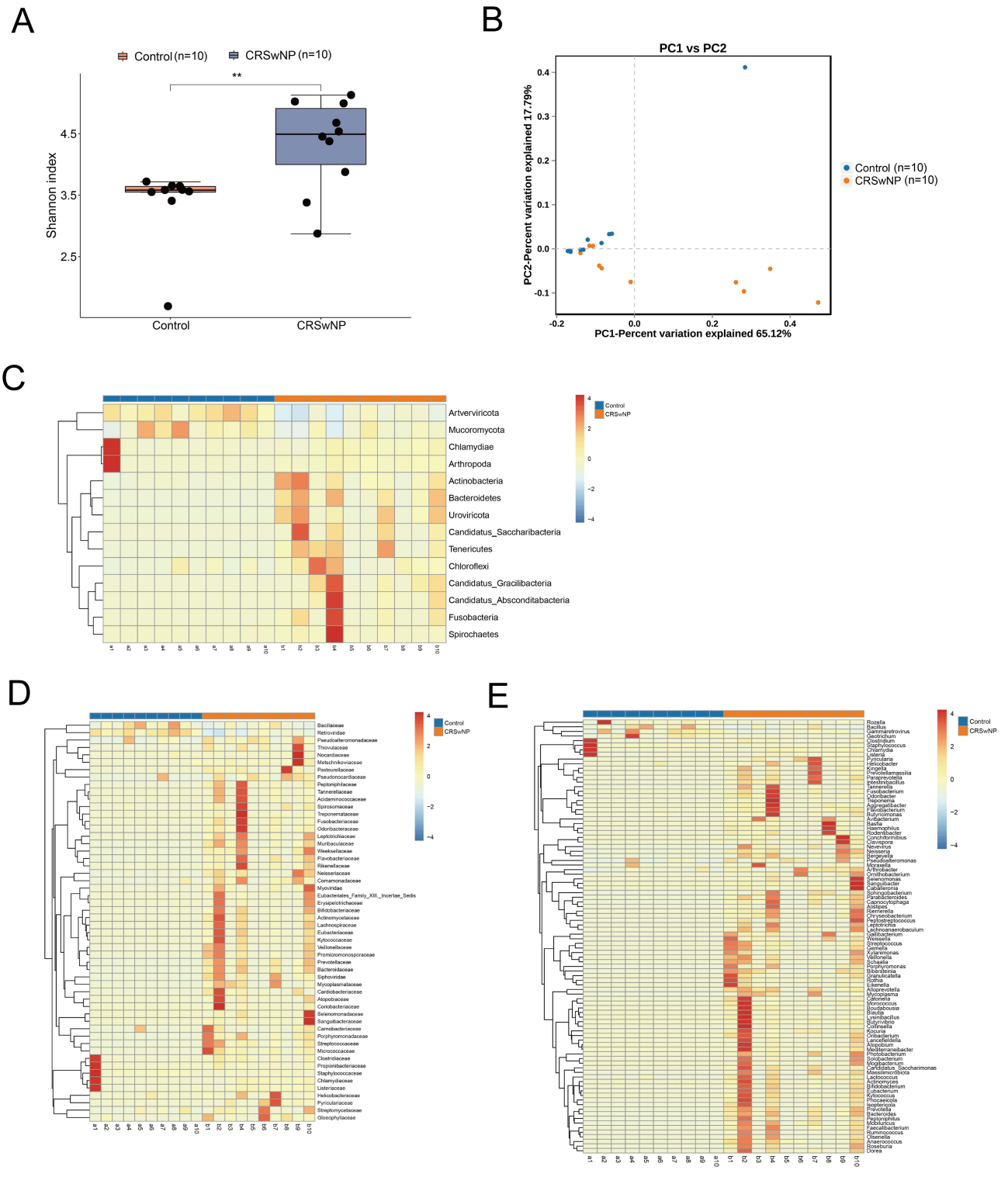

Figure 2 continued.

https://doi.org/10.2147/JIR.S567582

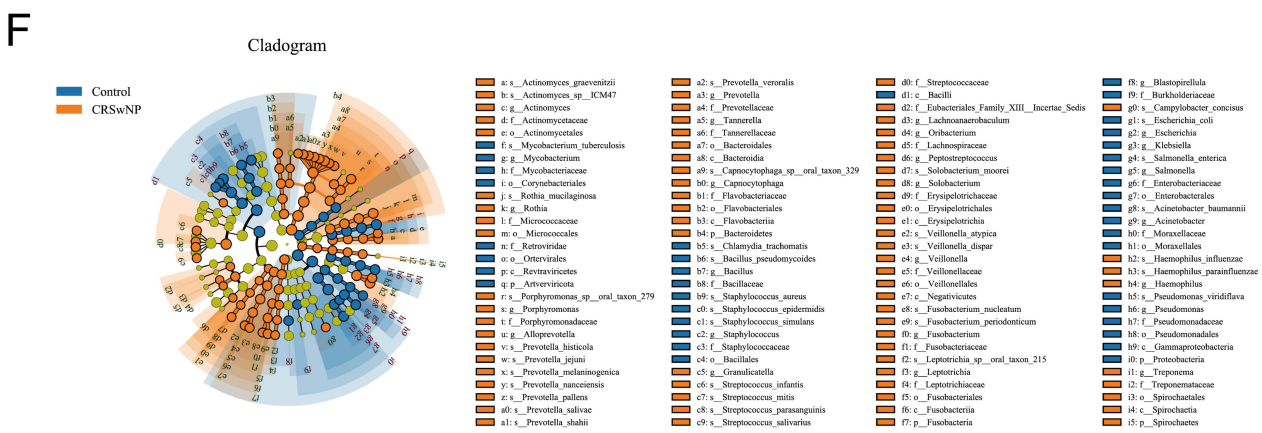

Figure 2 Nasal Microbial Communities in CRSwNP (n=10) and Control (n=10). (**A**) Shannon diversity index comparison (P<0.01). (**B**) PCoA plot based on species abundance (PC1 and PC2 account for 65.12% and 17.79% of variance). (**C**–**E**) Heatmaps of species abundance differences at phylum, genus, and family levels (Kruskal–Wallis test). (**F**) LEfSe cladogram of differentially abundant species.

Haemophilus, and *Fusobacterium* may have contributed to CRSwNP, so these 6 microbes were also included in the analysis. Finally, a one-to-one correlation analysis between the 62 metabolites and 21 microbial species (P<0.05) revealed 20 microbial species and 52 metabolites with direct correlations (Figure 4D and Table S11). In the CRSwNP group, *Streptococcus* was significantly positively correlated with 13′-Hydroxy-alpha-tocopherol.

Proteomics

In this study, proteomic sequencing was performed on 10 experimental group samples and 19 control group samples, and a total of 5620 proteins were quantified (Table S12). Among them, 735 proteins were differentially expressed, including 46 upregulated and 689 downregulated (Figure 5A, B and Table S13). GO functional analysis revealed 74 enriched pathways, including processes such as proteasomal protein catabolic process, glutathione metabolism, proteasome core complex, α-subunit complex, and pre-mRNA binding (Figure 5C and Table S14). KEGG functional enrichment analysis revealed significant enrichment in pathways related to glutathione metabolism, drug metabolism - cytochrome P450, spliceosome, chemical carcinogenesis, proteasome, and metabolism of xenobiotics by cytochrome P450 (p<0.05) (Figure 5D and Table S15).

Metabolomics and Proteomics Integrated Analysis

Correlation analysis was performed between the 55 proteins identified in the pathways from GO and KEGG enrichment analysis of differentially expressed proteins and the 52 metabolites directly associated with microorganisms. The analysis showed that 54 proteins were directly correlated with 49 metabolites ($|CC| > 0.4$, $P < 0.05$). Among the correlated pairs, 3 metabolites were positively associated with 48 proteins, and 47 metabolites were negatively associated with 49 proteins. Notably, two proteins involved in the glutathione metabolism pathway, GCLM and GGCT, exhibited particularly strong negative correlations with the metabolite 13′-Hydroxy-alpha-tocopherol (GCLM: $CC = -0.592$, $P = 0.00072$; GGCT: $CC = -0.526$, $P = 0.00338$). The integrated correlation network of metabolites and proteins is summarized in Table S16 and visualized in Figure 5E.

Discussion

This study found that, compared to the control group, children with CRSwNP exhibited greater nasal microbial diversity and significant differences in microbial populations: *Streptococcus*, *Bacteroides*, *Prevotella*, and *Haemophilus influenzae* were significantly upregulated. These findings are consistent with some previous studies, which suggest that the heterogeneity of CRS patients may be related to differences in bacterial microbiomes and host immune responses.[11,12] However, previous studies have not reached a consensus regarding microbial community diversity. A study by Mahajan et al found that children with CRS had higher nasal microbiome α-diversity compared to the control group;[13] however, in the study by Gan et al, adult CRSwNP patients had lower nasal microbiome richness than the control group, and there

https://doi.org/10.2147/JIR.S567582

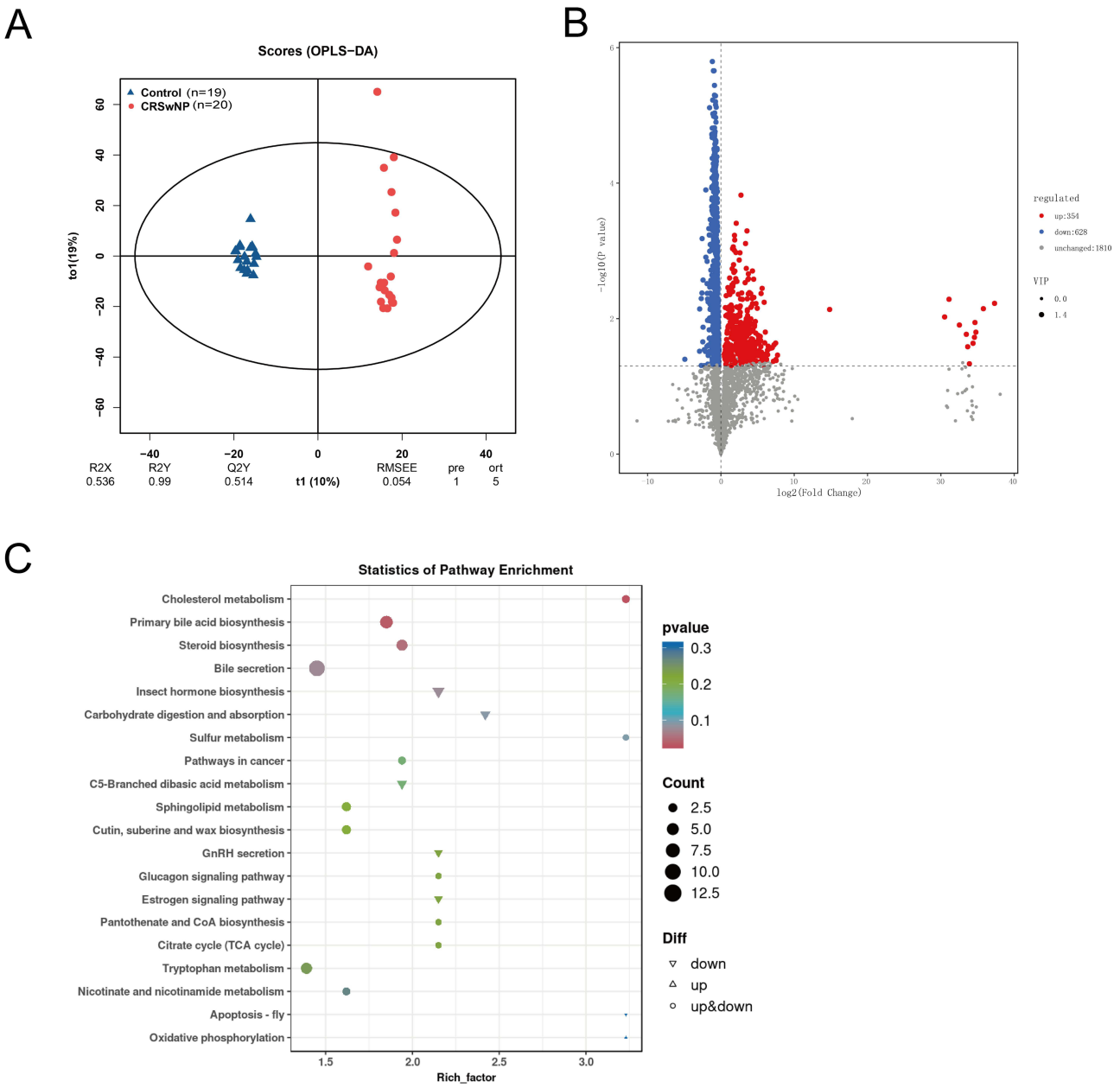

Figure 3 Metabolomic Features of Nasal Secretions in CRSwNP (n=20) and Control (n=19). (**A**) OPLS-DA score plot of metabolites. (**B**) Volcano plot of differentially expressed metabolites (red, upregulated; blue, downregulated in the CRSwNP group). (**C**) KEGG pathway enrichment of differential metabolites.

was no significant difference in community composition between the two groups.[14] *Streptococcus* is a common pathogen in respiratory diseases. Studies have found that during infection, *Streptococcus* catalyzes the conversion of pyruvate to acetyl phosphate, releasing CO_2 and H_2O_2 as by-products, in order to promote colonization and suppress the activity and virulence of competing pathogens.[15,16] After respiratory epithelial cells are infected by *Streptococcus*, they release cytokines and chemokines such as Interleukin 8 and Tumor Necrosis Factor-α, which attract inflammatory cells, primarily neutrophils, to gather at the site of infection. To suppress bacterial spread and infection, neutrophils release myeloperoxidase and large amounts of reactive oxygen species (ROS), including superoxide anion and hydrogen peroxide, which damage the cell membrane and other structures of *Streptococcus*.[17] Excessive ROS exacerbates epithelial cell damage, leading to an intensified local inflammatory response.[17]

https://doi.org/10.2147/JIR.S567582

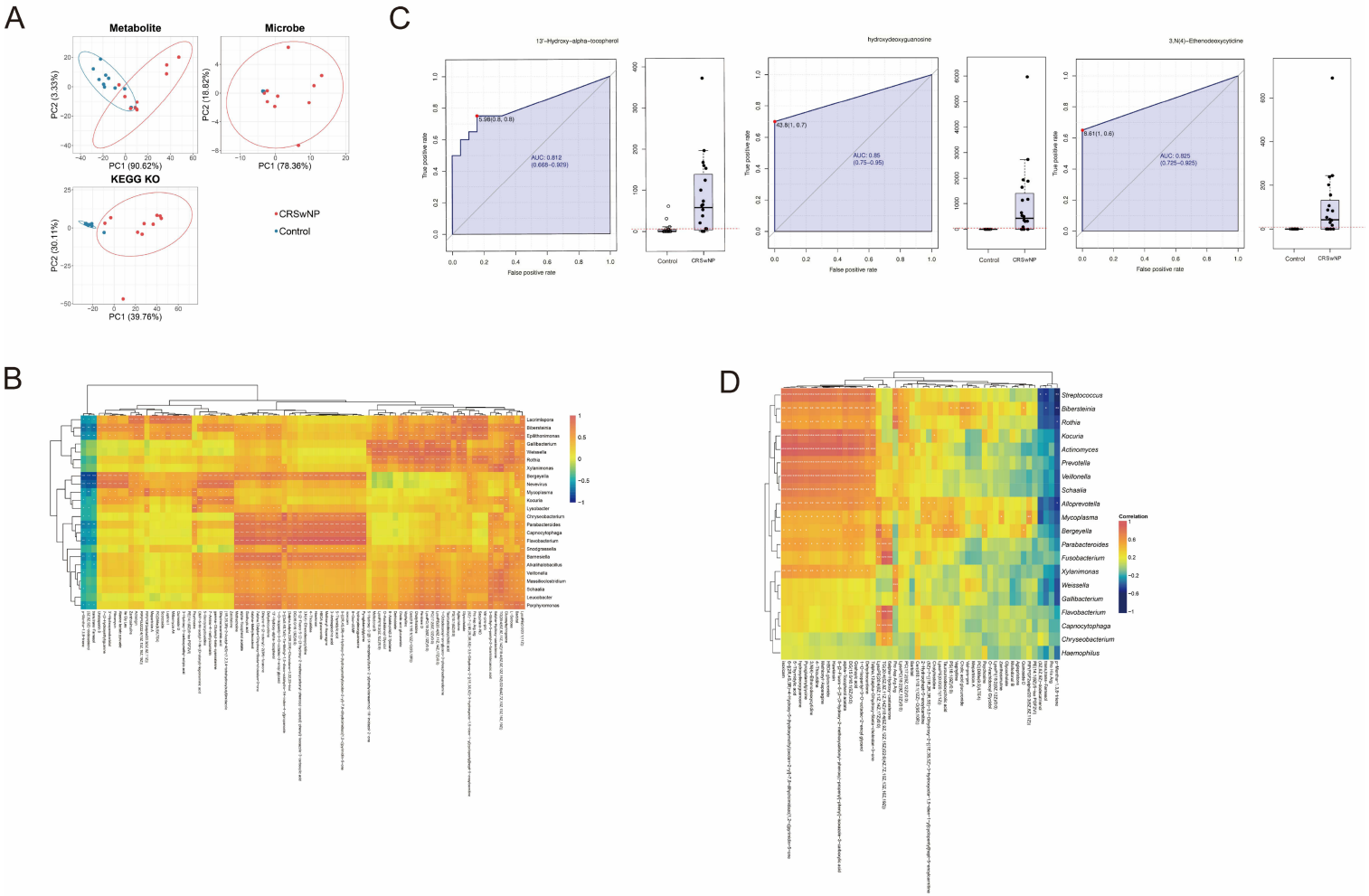

Figure 4 Integrated Analysis of Metagenomics and Metabolomics. (**A**) PCA of metagenomics and metabolomics data ("Metabolite": metabolomics; "Microbe": microbial composition; "KEGG KO": KEGG orthology genes). PC1 and PC2 represent major variance. (**B**) Clustering heatmap of microbe–metabolite correlations (CCP<0.05, |CC|>0.8). (**C**) ROC curve analysis of metabolites associated with differential microbes. (**D**) Heatmap of highly correlated microbe–metabolite pairs.

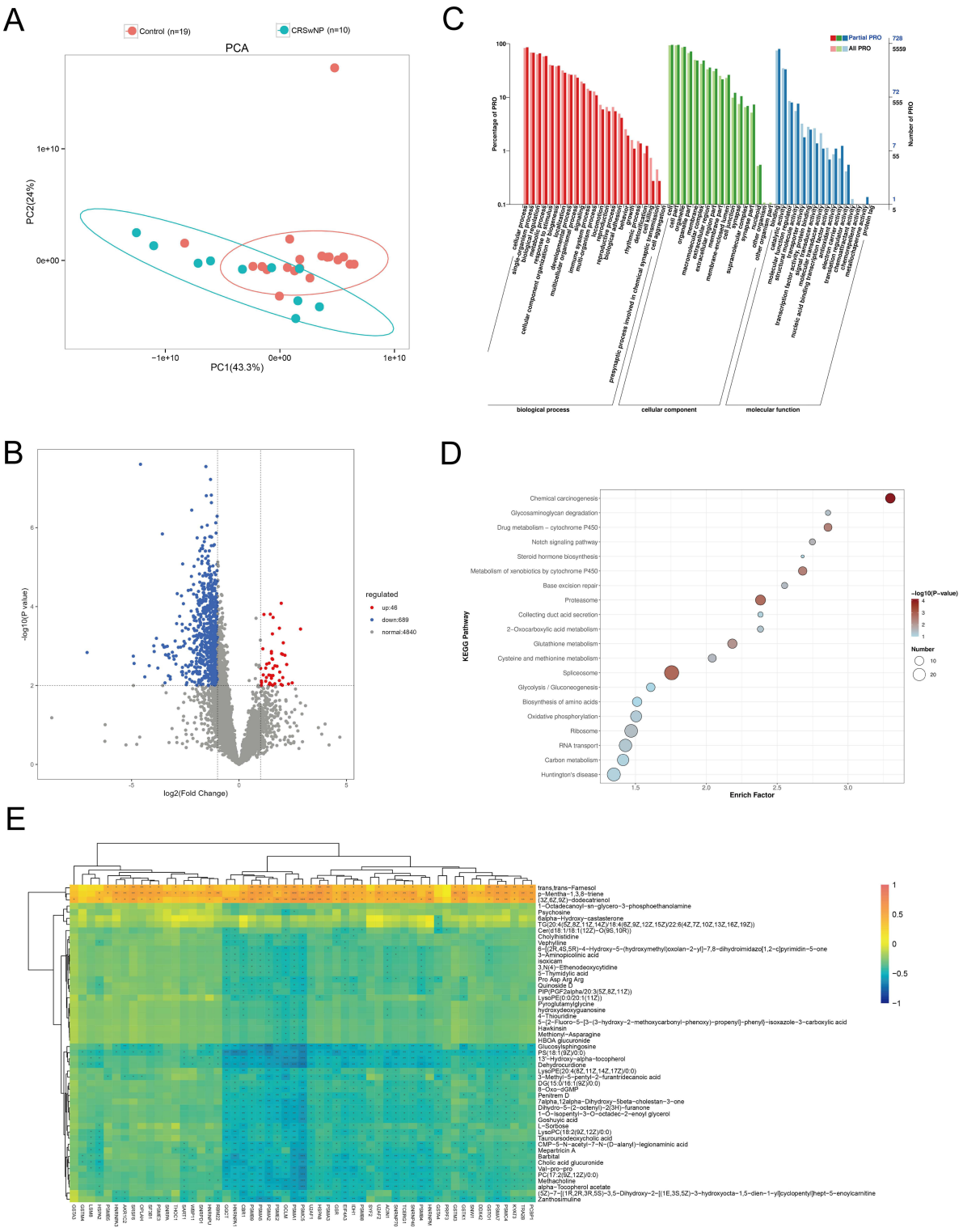

Figure 5 Protein Expression and Integrated Metabolomics-Proteomics Analysis in CRSwNP and Control. (**A**) PCA plot of protein expression data. (**B**) Volcano plot of differentially expressed proteins (red, upregulated; blue, downregulated in the CRSwNP group). (**C**) GO annotation of differential proteins. (**D**) KEGG pathway enrichment of differential proteins. (**E**) Heatmap of highly correlated metabolites and proteins.

Interestingly, we found that 13′-Hydroxy-alpha-tocopherol, which is involved in linoleic acid metabolism, was upregulated in the CRSwNP group. In the metabolic pathway of vitamin E, "long-chain metabolites" are formed, including 13′-hydroxy and subsequently oxidised 13′-carboxy derivatives.[18] 13′-Hydroxy- alpha -tocopherol is generated via hepatic ω-hydroxylation of the phytyl side chain followed by successive β-oxidation, while retaining the chromanol ring structure. As a lipophilic antioxidant, it can scavenge peroxyl free radicals during lipid oxidation, protecting polyunsaturated fatty acids from peroxidative damage and mitigating oxidative stress.[19] Recent studies suggest that these long-chain metabolites may exert stronger anti-inflammatory and redox-regulatory effects than the parent α-tocopherol, partly through modulation of inflammatory signaling and nuclear receptor activity. These metabolites have been implicated in the regulation of inflammatory signaling pathways, macrophage foam-cell formation, and nuclear receptor activation. Pein et al reported that the endogenous α-tocopherol metabolite α-tocopherol-13′-COOH possesses immunomodulatory and anti-inflammatory properties, effectively suppressing inflammation in mouse models of peritonitis and reducing airway hyperresponsiveness in asthma models.[20] Moreover, compared to the control group, the CRSwNP group showed significant upregulation of hydroxydeoxyguanosine and 3,N(4)-Ethenodeoxycytidine, both of which are markers of DNA oxidative damage, further suggesting that the development of CRSwNP is associated with oxidative stress.[21] Taken together, the biochemical characteristics of 13′-Hydroxy-alpha-tocopherol make it a plausible exploratory biomarker of oxidative imbalance in pediatric CRSwNP, warranting further validation in larger studies.

In our multi-omics analysis, we observed a strong correlation between *Streptococcus* and 13′-Hydroxy-alpha-tocopherol in the nasal secretions of CRSwNP patients. Additionally, 13′-Hydroxy-alpha-tocopherol was strongly negatively correlated with the proteins GCLM and GGCT, which are enriched in the glutathione metabolism pathway and significantly downregulated in the CRSwNP group. Glutathione metabolism is a crucial pathway for increasing intracellular Nicotinamide Adenine Dinucleotide Phosphate and reducing oxidative stress. GCLM is a component of the glutamate-cysteine ligase complex, the first rate-limiting enzyme in glutathione synthesis, catalyzing the formation of L-γ-glutamylcysteine from L-glutamate and L-cysteine, a key step in glutathione production.[22] γ-glutamyl cyclotransferase (GGCT) is involved in converting L-γ -glutamylcysteine to 5-oxoproline and L-cysteine. L-Cysteine availability is a critical determinant of GSH biosynthesis, thus influencing glutathione synthesis.[23] The downregulation of GCLM and GGCT severely disrupts glutathione synthesis, limiting the body's capacity to counter oxidative stress. Previous studies have shown that glutathione levels in CRSwNP patients are lower than those in normal nasal mucosa,[24] which is consistent with our findings.

Based on these findings, we propose a potential association between *Streptococcus* and oxidative stress in the nasal epithelium, possibly mediated by bacterial toxins and metabolic products.[25] ROS may contribute to local oxidative damage through free radical chain reactions.[26] Moreover, in the innate immune system, neutrophil antimicrobial activity also releases oxidative factors, further aggravating tissue damage.[27] The strong correlation between the upregulation of 13′-Hydroxy-alpha-tocopherol and the downregulation of GCLM and GGCT suggests a redox imbalance between peroxidation and antioxidation in the nasal microenvironment of children with CRSwNP.[24,28] Previous studies indicate that the development of pediatric CRSwNP also involves complex interactions between immune cells and inflammatory signaling pathways. Nasal polyp tissues often show prominent eosinophil infiltration and elevated Th2 cytokines such as IL-5 and IL-13,[29] while early disturbances in epithelial barrier integrity and microbial colonization may contribute to chronic inflammation and tissue remodeling.[30] Taken together, these findings suggest that pediatric CRSwNP arises from a multifactorial interplay among microbial dysbiosis, oxidative stress, and immune-mediated tissue remodeling. Therefore, 13′-Hydroxy-alpha-tocopherol may represent a plausible candidate small molecule biomarker in children with CRSwNP.

This study has certain limitations. Firstly, the abundance of Staphylococcus aureus in CRSwNP patients was relatively low in our findings, which may be attributed to factors affecting our sampling and sample preservation processes. Secondly, due to funding limitations, the sample size in this study was relatively small, which may affect statistical precision, but the findings still provide preliminary evidence on the microbial and metabolic features of pediatric CRSwNP. In addition, children with unilateral nasal bone fractures, no prior sinonasal symptoms, normal CT scans, and intraoperative endoscopic confirmation of intact nasal mucosa were selected as controls. Although trauma-related physiological stress may introduce minor variability, all samples were collected from the non-fractured side seven days post-injury under standardized anesthesia conditions, using identical sampling sites and storage protocols to

minimize potential bias. Moreover, although key demographic and clinical parameters were comparable between groups and standardized perioperative management was applied, the potential influence of unmeasured confounders cannot be entirely excluded. Finally, although our findings provide evidence for the interaction between the *Streptococcus*-13′-Hydroxy-alpha-tocopherol-glutathione metabolism pathway, further validation in independent cohorts is warranted. Future work will include targeted LC-MS/MS and PRM/SRM assays to validate candidate metabolites and proteins, together with in vitro nasal epithelial models and in vivo nasal inflammation models to test whether the *Streptococcus*–13′-Hydroxy-α-tocopherol–glutathione axis exerts functional effects.

Conclusion

This study utilized multi-omics integrated analysis to elucidate the correlation between *Streptococcus*, 13′-Hydroxy-alpha -tocopherol, and the glutathione metabolism pathway in nasal secretions of children with CRSwNP. It is speculated that the dysregulation of the oxidative and antioxidative defense processes in the nasal mucosal epithelium is an important molecular mechanism underlying the development of nasal polyps in children. The metabolite 13′-Hydroxy-alpha-tocopherol emerged as a potential small-molecule candidate of interest. These exploratory observations warrant independent validation to confirm its mechanistic relevance and biomarker potential in pediatric CRSwNP.

Abbreviations

CRSwNP, Chronic Rhinosinusitis with Nasal Polyps; FESS, Functional Endoscopic Sinus Surgery; LC-MS, Liquid Chromatography-Mass Spectrometry; OPLS-DA, Orthogonal Partial Least Squares Discriminant Analysis; DDA, Data-Dependent Acquisition; DIA, Data-Independent Acquisition; ROS, Reactive Oxygen Species; GGCT, γ-Glutamyl Cyclotransferase.

Data Sharing Statement

All data generated or analysed during this study are included in this published article and its supplementary information files. The original data supporting this study have been deposited in the Figshare repository and are openly available at https://doi.org/10.6084/m9.figshare.29617013.v1.

Ethics Approval

This article does not contain any studies with animals performed by any of the authors. This study was performed in line with the principles of the Declaration of Helsinki. Approval was granted by the Ethics Committee of Beijing Children's Hospital affiliated with Capital Medical University and the informed consent of all subjects ([2022]-E-215-Y). Prior to study commencement, written informed consent was obtained from the parents or legal guardians of all enrolled participants.

Author Contributions

Chao Jia and Xiaoge Liu are first authors. Chao Jia; Conceptualization, Methodology, Investigation, Data curation, Formal analysis, Visualization, Writing – original draft, Writing – review & editing. Xiaoge Liu; Conceptualization, Methodology, Investigation, Data curation, Formal analysis, Visualization, Writing – original draft, Writing – review & editing. Wenjing Liu; Investigation, Data curation, Methodology, Validation, Writing – review & editing. Xingfeng Yao; Investigation, Data curation, Methodology, Validation, Writing – review & editing. Xiaoxu Chen; Data curation, Validation, Resources, Project administration, Writing – review & editing. Jinhao Zhao; Data curation, Validation, Resources, Project administration, Writing – review & editing. Pengpeng Wang; Investigation, Data curation, Methodology, Project administration, Writing – review & editing. Wentong Ge; Supervision, Project administration, Funding acquisition, Resources, Writing – review & editing. Yang Han; Supervision, Project administration, Funding acquisition, Methodology, Resources, Writing – review & editing. All authors gave final approval of the version to be published; have agreed on the journal to which the article has been submitted; and agree to be accountable for all aspects of the work.

Funding

This work was supported by Beijing Natural Science Foundation (7242052); Training Fund for Open Projects at Clinical Institutes and Departments of Capital Medical University (CCMU2023ZKYXY001); Capital's Funds for Health Improvement and Research (2024-2-2098); Respiratory Research Project of National Clinical Research Center for Respiratory Diseases (HXZX-202109); Beijing Natural Science Foundation-Haidian Original Innovation Joint Fund (L232034); Special Projects for Organized Scientific Research at Chinese Institutes for Medical Research (CX23YZ10); and Capital's Funds for Health Improvement and Research (2024-1-2093).

Disclosure

The authors declare that they have no competing interests.

References

1. Snidvongs K, Sangubol M, Poachanukoon O. Pediatric versus adult chronic rhinosinusitis. *Curr Allergy Asthma Rep*. 2020;20(8):29. doi:10.1007/s11882-020-00924-6
2. Anamika A, Chakravarti A, Kumar R. Atopy and quality of life in pediatric chronic rhinosinusitis. *Am J Rhinol Allergy*. 2019;33(5):586–590. doi:10.1177/1945892419854266
3. Chegini Z, Noei M, Hemmati J, Arabestani MR, Shariati A. The destruction of mucosal barriers, epithelial remodeling, and impaired mucociliary clearance: possible pathogenic mechanisms of Pseudomonas aeruginosa and Staphylococcus aureus in chronic rhinosinusitis. *Cell Commun Signal*. 2023;21(1):306. doi:10.1186/s12964-023-01347-2
4. Loperfido A, Cavaliere C, Begvarfaj E, et al. The impact of antibiotics and steroids on the nasal microbiome in patients with chronic rhinosinusitis: a systematic review according to PICO criteria. *J Pers Med*. 2023;13(11):1583. doi:10.3390/jpm13111583
5. Park IH, Lee JS, Park JH, et al. Comparison of the human microbiome in adults and children with chronic rhinosinusitis. *PLoS One*. 2020;15(12):e0242770. doi:10.1371/journal.pone.0242770
6. Miller S, Naccache SN, Samayoa E, et al. Laboratory validation of a clinical metagenomic sequencing assay for pathogen detection in cerebrospinal fluid. *Genome Res*. 2019;29(5):831–842. doi:10.1101/gr.238170.118
7. Chen S, Zhou Y, Chen Y, Gu J. fastp: an ultra-fast all-in-one FASTQ preprocessor. *Bioinformatics*. 2018;34(17):i884–i90. doi:10.1093/bioinformatics/bty560
8. Li D, Liu CM, Luo R, Sadakane K, Lam TW. MEGAHIT: an ultra-fast single-node solution for large and complex metagenomics assembly via succinct de Bruijn graph. *Bioinformatics*. 2015;31(10):1674–1676. doi:10.1093/bioinformatics/btv033
9. Kim SH, Han DG, Shim JS, Lee YJ, Kim SE. Clinical characteristics of adolescent nasal bone fractures. *Arch Craniofac Surg*. 2022;23(1):29–33. doi:10.7181/acfs.2022.00038
10. Landeen KC, Kimura K, Stephan SJ. Nasal Fractures. *Facial Plast Surg Clin North Am*. 2022;30(1):23–30. doi:10.1016/j.fsc.2021.08.002
11. Cope EK, Goldberg AN, Pletcher SD, Lynch SV. Compositionally and functionally distinct sinus microbiota in chronic rhinosinusitis patients have immunological and clinically divergent consequences. *Microbiome*. 2017;5(1):53. doi:10.1186/s40168-017-0266-6
12. De Boeck I, Wittouck S, Martens K, et al. Anterior nares diversity and pathobionts represent sinus microbiome in chronic rhinosinusitis. *MSphere*. 2019;4(6). doi:10.1128/MSphere.00532-19
13. Mahajan E, Cheng J. A pilot investigation of the pediatric nasal microbiome. *Otolaryngol Head Neck Surg*. 2021;165(6):895–898. doi:10.1177/01945998211004161
14. Gan W, Yang F, Tang Y, et al. The difference in nasal bacterial microbiome diversity between chronic rhinosinusitis patients with polyps and a control population. *Int Forum Allergy Rhinol*. 2019;9(6):582–592. doi:10.1002/alr.22297
15. Tuomanen EI, Austrian R, Masure HR. Pathogenesis of pneumococcal infection. *New Engl J Med*. 1995;332(19):1280–1284. doi:10.1056/NEJM199505113321907
16. Wu X, Gordon O, Jiang W, et al. Interaction between *streptococcus pneumoniae* and *staphylococcus aureus* generates (·)OH radicals that rapidly kill staphylococcus aureus strains. *J Bacteriol*. 2019;201(21). doi:10.1128/JB.00474-19
17. Mraheil MA, Toque HA, La Pietra L, et al. Dual role of hydrogen peroxide as an oxidant in pneumococcal pneumonia. *Antioxid. Redox Signaling*. 2021;34(12):962–978. doi:10.1089/ars.2019.7964
18. Schubert M, Kluge S, Schmölz L, et al. Long-chain metabolites of vitamin e: metabolic activation as a general concept for lipid-soluble vitamins? *Antioxidants*. 2018;7(1):10. doi:10.3390/antiox7010010
19. Wallert M, Ziegler M, Wang X, et al. α-tocopherol preserves cardiac function by reducing oxidative stress and inflammation in ischemia/reperfusion injury. *Redox Biol*. 2019;26:101292. doi:10.1016/j.redox.2019.101292
20. Pein H, Ville A, Pace S, et al. Endogenous metabolites of vitamin E limit inflammation by targeting 5-lipoxygenase. *Nat Commun*. 2018;9(1):3834. doi:10.1038/s41467-018-06158-5
21. Lunec J, Holloway KA, Cooke MS, Faux S, Griffiths HR, Evans MD. Urinary 8-oxo-2'-deoxyguanosine: redox regulation of DNA repair in vivo? *Free Radic Biol Med*. 2002;33(7):875–885. doi:10.1016/S0891-5849(02)00882-1
22. Parvin S, Lee OR, Sathiyaraj G, Khorolragchaa A, Kim YJ, Yang DC. Spermidine alleviates the growth of saline-stressed ginseng seedlings through antioxidative defense system. *Gene*. 2014;537(1):70–78. doi:10.1016/j.gene.2013.12.021
23. Oakley AJ, Yamada T, Liu D, Coggan M, Clark AG, Board PG. The identification and structural characterization of C7orf24 as gamma-glutamyl cyclotransferase. An essential enzyme in the gamma-glutamyl cycle. *J Biol Chem*. 2008;283(32):22031–22042. doi:10.1074/jbc.M803623200
24. Mrowicka M, Zielinska-Blizniewska H, Milonski J, Olszewski J, Majsterek I. Evaluation of oxidative DNA damage and antioxidant defense in patients with nasal polyps. *Redox Rep*. 2015;20(4):177–183. doi:10.1179/1351000215Y.0000000001

25. Rai P, Parrish M, Tay IJ, et al. *Streptococcus pneumoniae* secretes hydrogen peroxide leading to DNA damage and apoptosis in lung cells. *Proc Natl Acad Sci USA*. 2015;112(26):E3421–30. doi:10.1073/pnas.1424144112
26. Gutteridge JM. Lipid peroxidation and antioxidants as biomarkers of tissue damage. *Clin. Chem*. 1995;41(12 Pt 2):1819–1828. doi:10.1093/clinchem/41.12.1819
27. van der Veen BS, de Winther MP, Heeringa P. Myeloperoxidase: molecular mechanisms of action and their relevance to human health and disease. *Antioxid. Redox Signaling*. 2009;11(11):2899–2937. doi:10.1089/ars.2009.2538
28. Zhou J, Zhou J, Liu R, et al. The oxidant-antioxidant imbalance was involved in the pathogenesis of chronic rhinosinusitis with nasal polyps. *Front Immunol*. 2024;15:1380846. doi:10.3389/fimmu.2024.1380846
29. Jiang L, Zeng Y, Huang Z, et al. Immunopathologic characteristics of Chinese pediatric patients with chronic rhinosinusitis. *World Allergy Organ J*. 2021;14(12):100616. doi:10.1016/j.waojou.2021.100616
30. Brown HJ, Khalife S, Ganesan V, et al. Histopathologic differences between adult and pediatric patients with chronic rhinosinusitis. *Int Forum Allergy Rhinol*. 2023;13(1):25–30. doi:10.1002/alr.23037